Rydberg mediated entanglement in a two-dimensional neutral atom qubit array

T. M. Graham, M. Kwon, B. Grinkemeyer, Z. Marra, X. Jiang, M. T. Lichtman,* Y. Sun,† M. Ebert,‡ and M. Saffman‡

Department of Physics, University of Wisconsin-Madison,
1150 University Avenue, Madison, Wisconsin 53706
(Dated: August 20, 2019)

We demonstrate high fidelity two-qubit Rydberg blockade and entanglement in a two-dimensional qubit array. The qubit array is defined by a grid of blue detuned lines of light with 121 sites for trapping atomic qubits. Improved experimental methods have increased the observed Bell state fidelity to $F_{\text{Bell}} = 0.86(2)$. Accounting for errors in state preparation and measurement (SPAM) we infer a fidelity of $F_{\text{Bell}}^{-\text{SPAM}} = 0.89$. Including errors in single qubit operations we infer that the Rydberg mediated C_Z gate has a fidelity of $F_{C_Z}^{-\text{SPAM}} = 0.91$. Comparison with a detailed error model shows that further improvement in fidelity will require colder atoms and lasers with reduced noise.

Achieving the promise of a computational advantage for quantum machines is predicated on the development of approaches that combine a large number of qubits with a high fidelity universal gate set. A broad range of experimental platforms for quantum computing are being developed[1] and very high fidelity two-qubit gates have been implemented in trapped ion and superconducting systems with small numbers of qubits: $F_{\text{Bell}} \geq 0.999$ with two trapped ions[2] and a phase gate fidelity $F_{C_z} > 0.99$ with five superconducting qubits[3]. As the number of qubits in a quantum computer is scaled up, crosstalk and undesired interactions may limit fidelity. Average Bell state fidelities of $F_{\text{Bell}} = 0.975$ were obtained in an 11 qubit ion trap[4]. An approach based on qubits encoded in hyperfine states of optically trapped neutral atoms holds great promise for scaling the number of qubits without limiting gate fidelities. The physical attribute that enables scaling with low crosstalk is the separation by 12 orders of magnitude between the weak coupling strength of neutral atom hyperfine qubits, and the strong interactions of Rydberg excited atoms[5] that are used to realize entangling gates[6]. We report here on experimental progress in achieving high entanglement fidelity in a 2D array of more than 100 qubits. The intrinsic gate fidelity of $F_{C_z} = 0.91$ we report here, together with previously demonstrated single qubit gates with $F > 0.99$[7, 8], and atom rearrangement capabilities[9] suggest that neutral atom arrays will soon be capable of advancing the state of the art in gate based quantum computing.

A computationally universal set of quantum gates can be built from one- and two-qubit operations. High fidelity one-qubit gates with fidelities determined by randomized benchmarking exceeding 0.99 and crosstalk to other sites less than 0.01 have been demonstrated in 2D[7]

* Present address: Joint Quantum Institute and Department of Physics, University of Maryland, College Park, MD 20742
† Present address: Interdisciplinary Center for Quantum Information, National University of Defense Technology, Changsha 410073, China
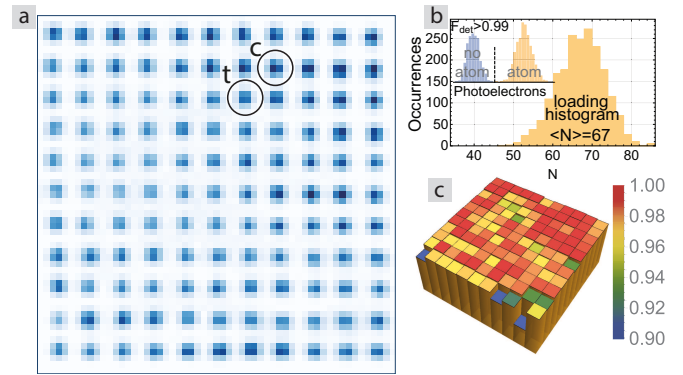‡ ColdQuanta, Inc., 811 E. Washington Ave, Suite 408, Madison, WI 53703

FIG. 1. (color online) Atomic qubit array. a) Averaged fluorescence image of 121 site array after ICA processing with the control and target sites used for the presented data labeled. b) Loading histogram with inset showing state detection inferred after blow away of atoms in $f = 4$. c) Atom retention probability after measurement. Accounting for all 121 sites the state detection error found from the overlap of Gaussians fitted to the $|0\rangle$ and $|1\rangle$ distributions was mean= 0.014, median= 0.003. The atom retention probability was mean= 96.9%, median= 97.9%.

and 3D[8] arrays of neutral atom qubits. However the fidelity of two-qubit entangling gates has been limited to much lower values. The highest fidelity results from the last few years for entanglement of pairs of neutral atoms are 0.79[10], 0.81[11], 0.59[12], 0.81[13]. These fidelity numbers are corrected for SPAM errors and in some cases also atom loss. Recent progress with qubits encoded in one hyperfine ground state and one Rydberg state has demonstrated entanglement fidelity of 0.97[14], although the use of Rydberg encoding limits the coherence time to < 0.1 ms, which is much shorter than the seconds of coherence time that have been achieved with qubits encoded in hyperfine ground states[8, 15].

The experimental setup is an upgraded version of that described in [10]. A two-dimensional array of Cs atoms is prepared using a projected optical lattice with period $d = 3.1(1)$ μm (numbers in parentheses are uncertainties in the last digit) and wavelength $\lambda = 825$ nm. (see Fig.1). In contrast to our previous work with a Gaussian
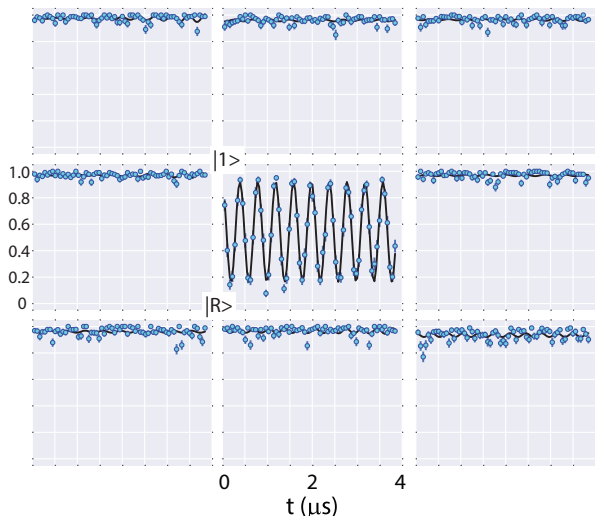
FIG. 2. (color online) Single site ground-Rydberg Rabi oscillations at $\Omega_R/2\pi = 2.5$ MHz with negligible crosstalk to the surrounding eight sites.

beam array[16], the array structure is defined by a square grid of lines of light that are prepared using diffractive optical elements[17]. Each unit cell provides 3D atom confinement with the transverse localization due to the repulsive walls of blue-detuned light, and axial confinement perpendicular to the plane of the array provided by diffractive spreading of the lines. We measure vacuum limited lifetimes of ~ 30 s, longitudinal coherence times in the Cs clock states of $T_1 = 0.75$ s and an average temperature of $T_a \simeq 15\,\mu$K. The atomic temperature implies a limit on the clock state coherence time due to motional variation of the trap light intensity of $T_2^* = 1.6$ ms.

The array is prepared by combining four laser sources with different frequencies such that the four beams defining each unit cell are separated by many MHz, but the frequencies are repeated in neighboring cells. With this configuration the structure and position of each trapping site are insensitive to phases caused by variations in optical path length which provides a very stable array. However, Talbot interference still occurs leading to additional trapping planes at axial separations of $L = 2(2d)^2/\lambda = 93\,\mu$m. Detection of atoms in the array is hampered by a diffuse background of scattering from atoms in the additional Talbot planes. We effectively reduce the background noise with regions of interest for each trap site, that are determined using an independent component analysis (ICA) algorithm[17], see Fig. 1. Alternatively the Talbot planes can be eliminated by making each line a different frequency. We have implemented this using acousto-optic deflectors to create the lines and thereby generated arrays with up to 196 trapping sites and an average of 110 trapped atoms. Details of this approach will be given elsewhere[18].

The trapped Cs atoms are optically pumped into the clock states which form a qubit basis of $|0\rangle = |6s_{1/2}, f = 3, m_f = 0\rangle$ and $|1\rangle = |6s_{1/2}, f = 4, m_f = 0\rangle$. State $|1\rangle$ is resonantly coupled to the Rydberg state $|R\rangle = |66s_{1/2}, m_j = -1/2\rangle$ using a two-photon transition with counterpropagating $\lambda_1 = 459$ nm (σ_+) and $\lambda_2 = 1038$ nm (σ_-) laser beams which couple $6s_{1/2} \to 7p_{1/2} \to 66s_{1/2}$. We detune by $+680$ MHz from the center of mass of the $7p_{1/2}$ state and use a magnetic bias field of 0.6 mT directed along the quantization axis, which is collinear with the beam $\mathbf{k}$ vectors, to separate the Rydberg $m_j = \pm 1/2$ states. The choice of Rydberg principal quantum number is lower than in our previous demonstrations and is desirable for minimizing perturbations from background electric fields. With the small array period used here there is sufficient blockade strength and state lifetime at $n = 66$ that the resulting errors are minor contributions to the overall error model (see Table I below).

The Rydberg excitation beams are focused to beam waists ($1/e^2$ intensity radii) of $w_1 = w_2 = 3.0\,\mu$m which are pointed to address desired sites in the array using crossed acousto-optic modulators for each beam. Figure 2 shows ground to Rydberg Rabi oscillation data in the array. The trap light is turned off during the Rydberg pulse. Since the blue detuned array traps Rydberg atoms when turned on again[19, 20] there is only minimal mechanical loss of Rydberg states. In order to detect Rydberg excitation we turn on a short 9.2 GHz microwave pulse (duration 70 μs) to photoionize the Rydberg atom. Rydberg detection efficiencies are typically 80-90%. The data was obtained using diode lasers that are stabilized to high finesse optical resonators (~ 5 kHz linewidth) with ultralow expansion mirror spacers placed in temperature controlled vacuum cans. The linewidths of the lasers determined by beating two such lasers together were determined to be under 300 Hz. It has been recognized that phase noise of diode lasers contributes to decay of ground-Rydberg oscillations[21], with improved performance achieved by resonator filtering[14]. Here we demonstrate comparable performance, without any resonator filtering, but with careful tuning of the electronic Pound-Drever-Hall lock parameters to reduce the amplitude of servo bumps.

The nominal Rabi frequency at neighboring sites due to Rydberg beam crosstalk is $\Omega_R' = e^{-d^2/w_1^2} e^{-d^2/w_2^2} \Omega_R = 0.12\,\Omega_R$, while the data shows no evidence of Rabi oscillations at the other sites. We achieve reduced crosstalk by using beam powers that give a nonzero differential Stark shift of $\Delta'/2\pi = 2$ MHz between ground and Rydberg states which suppresses the oscillation amplitude to $(\Omega_R'/\Delta')^2 = 0.023$.

A curve fit to the Rabi oscillations at the selected site in Fig. 2 does not reveal a statistically significant decay time. The radiative lifetime of the 66s state is 130 μs and the motional dwell time of a Rydberg atom in a trap site is $\sim 50\,\mu$s. Both time constants are much longer than the observed 4 μs of coherent oscillations. However, the ground-Rydberg phase coherence decays due to Doppler sensitivity of the two-photon excitation according to[22] $\langle e^{i\phi} \rangle = e^{-t^2/T_{2,\mathrm{D}}^2}$ with $T_{2,\mathrm{D}} = \sqrt{2M_{\mathrm{Cs}}/k_B T_a}/k_{2\nu}$ and $k_{2\nu} = 2\pi/\lambda_1 - 2\pi/\lambda_2$. At $T_a = 15\,\mu$K we find $T_{2,\mathrm{D}} = 6\,\mu$s
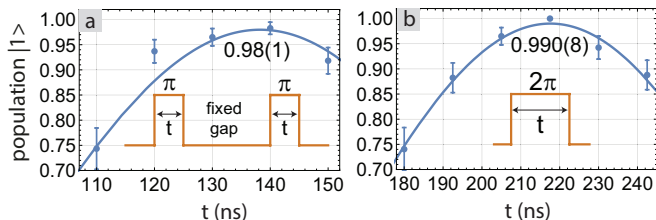
FIG. 3. (color online) Population in $|1\rangle$ after a) control and b) target qubit Rydberg pulses. The Rabi frequencies for the control and target pulses were $\Omega_R/2\pi = 3.6$ and 4.6 MHz respectively and gap time = 300 ns.

FIG. 4. (color online) Eye diagram for target qubit with blockade and no-blockade curves of amplitude 0.91(6) and 0.85(3). The inset shows the target pulse sequence. The C_Z gate was operated at $\theta = 0.95$ radians.

which would seem to imply a noticeable decay of the Rabi amplitude. This is not the case because the effective coherence, or persistence time, of a driven oscillation is much longer than that of a static superposition of states.

The original proposal for a Rydberg C_Z gate[6] involves a sequence of three pulses connecting ground and Rydberg states: a π pulse on the control qubit, 2π on the target qubit, and π on the control qubit. It has been shown by detailed analysis of the atomic structure of the heavy alkalis that this pulse sequence is in principle capable of creating entanglement with fidelity $F > 0.998$ [23]. Many other Rydberg gate protocols have been proposed(see [24] for an overview). Using shaped pulses $F > 0.9999$ at gate times as short as 50 ns[25] appears possible. The infidelity of our current implementation is dominated by technical errors and finite atomic temperature, as opposed to intrinsic atomic structure parameters, and we report here on improved performance of the original proposal, leaving demonstration of alternative protocols for future work.

One of the technical errors that has been improved on is the loss of Rydberg atoms after the $\pi - gap - \pi$ pulses on the control qubit or the 2π pulse on the target qubit. These losses dominated the error budget in most earlier experiments[10, 26, 27]. With improvements to laser noise, optical beam quality, and alignment we have reduced population losses to 2% as shown in Fig. 3. In order to minimize excitation of Rydberg hyperfine states with $m_f \neq 0$ we align the **k** vectors of the 459 and 1038 nm beams to be anti-parallel and set the background magnetic fields and polarization of the 459 nm beam to be accurately σ_+ relative to a quantization axis along **k**. This is done by preparing the state $|4, 4\rangle$ and minimizing the scattering rate due to the 459 nm light. In addition for the data in Figs. 3 - 5 the beam waists were reduced slightly compared to those used for the data in Fig. 2 to $w_1 = 2.25$ μm and $w_2 = 2.5$ μm in order to minimize crosstalk between sites.

The next step in tuning the gate sequence is to verify the qubit phase induced by a 2π Rydberg pulse. We do this using a Ramsey sequence of $\pi/2$ - gap - $\pi/2$ pulses on the qubit states and insert a 2π $|1\rangle - |R\rangle$ pulse on the target qubit inside the gap as shown in Fig. 4. Performing this sequence with and without first exciting the control qubit to $|R\rangle$ with a π pulse gives an "eye" diagram that
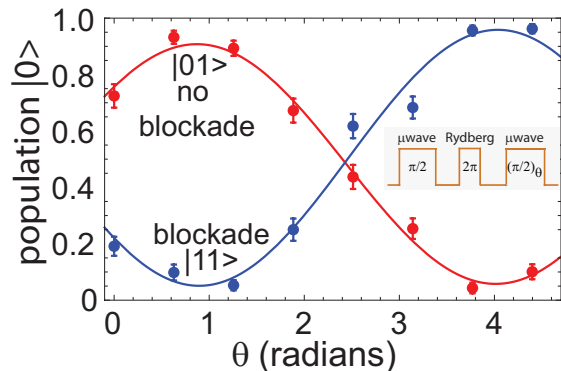
ideally consists of blockade and no-blockade curves that are π out of phase with each other. In the experiment these curves have a relative phase that is not equal to π due to Stark shifts of the qubit states induced by the Rydberg excitation beams[10]. To compensate for this we slightly detune the Rydberg pulse on the target to give the opposite phase Ramsey curves seen in the figure.

The observed amplitude of the blockade and no-blockade curves in Fig. 4 is 0.91(6) and 0.85(3). To prepare a maximally entangled Bell state with the C_Z gate the input state is $(|00\rangle + |10\rangle + |01\rangle + |11\rangle)/2$. The $|0\rangle$ state is not Rydberg coupled and is not affected by the gate sequence therefore $|00\rangle$ experiences no error, $|10\rangle$ corresponds to Fig. 3a), $|01\rangle$ corresponds to the no-blockade eye diagram curve, and $|11\rangle$ the blockaded eye diagram curve. It follows that the data in Fig. 3, 4 imply a limit on the fidelity of the output Bell state of $F_{max} = (1 + 0.98 + 0.89 + 0.88)/4 = 0.94$. The observed F_{Bell} is lower than F_{max} by an additional 0.08 which we attribute to the error channels discussed below in connection wtih Table I.

To prepare a Bell state we start with control and target qubits in $|c\rangle = |1\rangle$, $|t\rangle = |1\rangle$. We then perform the pulse sequence shown in Fig.5 which puts the control qubit in a superposition of $|0\rangle$ and $|1\rangle$ and implements a CNOT gate consisting of a target $\pi/2$ rotation, the C_Z Rydberg pulses, and a target $\pi/2$ rotation at angle θ. The populations of the two-qubit output state are measured, and the coherence is determined from the amplitude of parity oscillations due to a $\pi/2$ rotation at variable angle ϕ[10]. The resulting data shown in Fig. 5 gives $(P_{00} + P_{11})/2 = 0.47(2)$, parity amplitude $C = 0.391(6)$, and $F_{Bell} = 0.47 + 0.39 = 0.86(2)$.

The observed Bell fidelity can be understood from the error sources enumerated in Table I. The errors are divided into three categories: a) errors due to atomic parameters and finite temperature, b) errors in the single qubit operations used for the CNOT gate and parity measurement, and c) SPAM errors. Calculations and measurements supporting the error model are provided

TABLE I. Error budget for Rydberg C_Z gate and Bell state preparation using parameters from the Bell state experiment. The listed error values are for two atoms averaged over the four computational basis states. Supporting calculations and measurements for the error values are provided in the supplementary material[28].

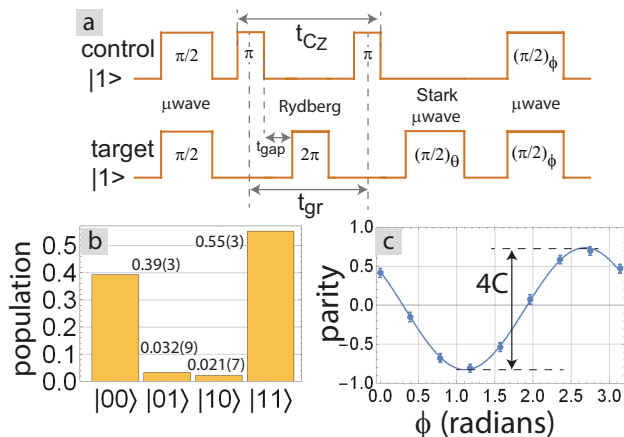| quantity	error	fidelity estimate
a) atomic parameters & finite temperature effects		
a.1) ground-Rydberg Doppler dephasing (calculated)	0.013	
a.2) Rydberg radiative lifetime (calculated)	0.004	
a.3) Rydberg motional dwell time (calculated)	0.014	
a.4) scattering $7p_{1/2}$ (calculated)	0.004	
a.5) blockade leakage (calculated)	0.001	
a.6) atom position in Rydberg beams (calculated)	0.035	
a.7) laser noise (estimated)	0.02	
	total 0.092	$F_{C_Z}^{-\text{SPAM}} = 0.908$
b) single qubit errors		
b.1) initial and parity global μwave pulses (measured)	0.008	
b.2) Stark μwave pulse (measured)	0.012	
	total 0.020	$F_{\text{Bell}}^{-\text{SPAM}} = 0.888$
c) SPAM errors		
c.1) atom preparation (measured)	0.01	
c.2) optical pumping (estimated)	0.01	
c.3) state measurement (measured)	3.0×10^{-4}	
	total 0.020	$F_{\text{Bell}} = 0.868$

FIG. 5. (color online) Bell state preparation: a) pulse sequence, b) populations, c) parity oscillation. The Rydberg pulses had lengths of $t_\pi = 150$ ns, $t_{2\pi} = 220$ ns, $t_{\text{gap}} = 300$ ns. The effective ground-Rydberg superposition time is $t_{\text{gR}} = t_\pi/2 + t_{\text{gap}} + t_{2\pi} + t_{\text{gap}} + t_\pi/2 = 0.98$ μs. The microwave pulses are global (duration 35 μs) for the initial and parity pulses and global pulses combined with a 459 nm Stark pulse (duration 70 μs) for the site selected rotation.

in the supplementary material[28]. We emphasize that this analysis is heuristic and is based on assigning estimated error values to physically distinct error mechanisms. Since the errors are not independent we have combined them linearly. Combining the errors in quadrature gives error estimates roughly twice smaller that do not agree well with measured data, both as regards the Bell state, and as regards measurements of fidelities for individual qubit operations. Including all errors we arrive at the value in the last line of Table I which is consistent

with the observed $F_{\text{Bell}} = 0.86(2)$. Accounting for SPAM errors gives a corrected Bell fidelity $F_{\text{Bell}}^{-\text{SPAM}} = 0.89$. Accounting for single qubit errors that go into the CNOT gate and parity measurements we arrive at a SPAM corrected value for the Rydberg C_Z gate of $F_{\text{C}_Z}^{-\text{SPAM}} = 0.91$.

It is apparent from the Table that the dominant C_Z gate error sources are due to finite temperature which leads to atomic motion and dephasing, and atomic position variations in the optical traps. In addition laser intensity and phase noise contribute to the gate error at the few percent level. The atomic structure errors that arise from the finite radiative lifetime of excited states and finite blockade strength contribute less than 1% to the error budget. These observations support the potential for the Rydberg interaction to mediate gates that have fidelity compatible with fault tolerant error correction after further technical improvements for reduced atom temperature and laser noise reduction.

In summary we have demonstrated a two-qubit Rydberg C_Z gate with intrinsic fidelity after correcting for SPAM and single qubit errors of $F_{C_Z}^{-\text{SPAM}} = 0.91$. The gate was used to prepare Bell states with observed fidelity of $F_{\text{Bell}} = 0.86(2)$ and SPAM corrected fidelity of $F_{\text{Bell}}^{-\text{SPAM}} = 0.89$. These fidelities were obtained with a 2D qubit array and using a tightly focused control beam geometry that is compatible with site specific gate operations across the array.

During the completion of our manuscript we became aware of related work demonstrating parallel operation of Rydberg gates[29].

[1] T. D. Ladd, F. Jelezko, R. Laflamme, Y. Nakamura, C. Monroe, and J. L. O'Brien, "Quantum computers," Nature **464**, 45 (2010).

[2] C. J. Ballance, T. P. Harty, N. M. Linke, M. A. Sepiol, and D. M. Lucas, "High-fidelity quantum logic gates using trapped-ion hyperfine qubits," Phys. Rev. Lett. **117**, 060504 (2016); J. P. Gaebler, T. R. Tan, Y. Lin, Y. Wan, R. Bowler, A. C. Keith, S. Glancy, K. Coakley, E. Knill, D. Leibfried, and D. J. Wineland, "High-fidelity universal gate set for ^{9}Be$^+$ ion qubits," *ibid.* **117**, 060505 (2016).

[3] R. Barends, J. Kelly, A.Megrant, A. Veitia, D.Sank, E. Jeffrey, T. C.White, J. Mutus, A. G. Fowler, B.Campbell, Y. Chen, Z. Chen, B. Chiaro, A. Dunsworth, C. Neill, P. OMalley, P. Roushan, A. Vainsencher, J. Wenner, A. N. Korotkov, A. N. Cleland, and J. M. Martinis, "Superconducting quantum circuits at the surface code threshold for fault tolerance," Nature **508**, 500 (2014).

[4] K. Wright, K. M. Beck, S. Debnath, J. M. Amini, Y. Nam, N. Grzesiak, J.-S. Chen, N. C. Pisenti, M. Chmielewski, C. Collins, K. M. Hudek, J. Mizrahi, J. D. Wong-Campos, S. Allen, J. Apisdorf, P. Solomon, M. Williams, A. M. Ducore, A. Blinov, S. M. Kreikemeier, V. Chaplin, M. Keesan, C. Monroe, and J. Kim, "Benchmarking an 11-qubit quantum computer," arXiv:1903.08181 (2019).

[5] M. Saffman, T. G. Walker, and K. Mølmer, "Quantum information with Rydberg atoms," Rev. Mod. Phys. **82**, 2313 (2010).

[6] D. Jaksch, J. I. Cirac, P. Zoller, S. L. Rolston, R. Côté, and M. D. Lukin, "Fast quantum gates for neutral atoms," Phys. Rev. Lett. **85**, 2208–2211 (2000).

[7] T. Xia, M. Lichtman, K. Maller, A. W. Carr, M. J. Piotrowicz, L. Isenhower, and M. Saffman, "Randomized benchmarking of single-qubit gates in a 2D array of neutral-atom qubits," Phys. Rev. Lett. **114**, 100503 (2015).

[8] Y. Wang, A. Kumar, T.-Y. Wu, and D. S. Weiss, "Single-qubit gates based on targeted phase shifts in a 3D neutral atom array," Science **352**, 1562 (2016).

[9] M. Endres, H. Bernien, A. Keesling, H. Levine, E. R. Anschuetz, A. Krajenbrink, C. Senko, V. Vuletic, M. Greiner, and M. D. Lukin, "Atom-by-atom assembly of defect-free one-dimensional cold atom arrays," Science **354**, 1024 (2016); D. Barredo, S. de Leséléuc, V. Lienhard, T. Lahaye, and A. Browaeys, "An atom-by-atom assembler of defect-free arbitrary two-dimensional atomic arrays," *ibid.* **354**, 1021 (2016); Aishwarya Kumar, Tsung-Yao Wu, Felipe Giraldo, and David S. Weiss, "Sorting ultracold atoms in a three-dimensional optical lattice in a realization of Maxwells demon," Nature **561**, 83 (2018); Daniel Barredo, Vincent Lienhard, Sylvain de Leséléuc, Thierry Lahaye, and Antoine Browaeys, "Synthetic three-dimensional atomic structures assembled atom by atom," *ibid.* **561**, 79 (2018).

[10] K. Maller, M. T. Lichtman, T. Xia, Y. Sun, M. J. Piotrowicz, A. W. Carr, L. Isenhower, and M. Saffman, "Rydberg-blockade controlled-NOT gate and entanglement in a two-dimensional array of neutral-atom qubits," Phys. Rev. A **92**, 022336 (2015).

[11] Y.-Y. Jau, A. M. Hankin, T. Keating, I. H. Deutsch, and G. W. Biedermann, "Entangling atomic spins with a Rydberg-dressed spin-flip blockade," Nat. Phys. **12**, 71 (2016).

[12] Yong Zeng, Peng Xu, Xiaodong He, Yangyang Liu, Min Liu, Jin Wang, D. J. Papoular, G. V. Shlyapnikov, and Mingsheng Zhan, "Entangling two individual atoms of different isotopes via rydberg blockade," Phys. Rev. Lett. **119**, 160502 (2017).

[13] C. J. Picken, R. Legaie, K. McDonnell, and J. D. Pritchard, "Entanglement of neutral-atom qubits with long ground-Rydberg coherence times," Quant. Sci. Technol. **4**, 015011 (2019).

[14] H. Levine, A. Keesling, A. Omran, H. Bernien, S. Schwartz, A. S. Zibrov, M. Endres, M. Greiner, V. Vuletić, and M. D. Lukin, "High-fidelity control and entanglement of Rydberg-atom qubits," Phys. Rev. Lett. **121**, 123603 (2018).

[15] Cheng Sheng, Xiaodong He, Peng Xu, Ruijun Guo, Kunpeng Wang, Zongyuan Xiong, Min Liu, Jin Wang, and Mingsheng Zhan, "High-fidelity single-qubit gates on neutral atoms in a two-dimensional magic-intensity optical dipole trap array," Phys. Rev. Lett. **121**, 240501 (2018).

[16] M. J. Piotrowicz, M. Lichtman, K. Maller, G. Li, S. Zhang, L. Isenhower, and M. Saffman, "Two-dimensional lattice of blue-detuned atom traps using a projected Gaussian beam array," Phys. Rev. A **88**, 013420 (2013).

[17] M. T. Lichtman, "Coherent operations, entanglement, and progress towards quantum search in a large 2D array of neutral atom qubits," PhD thesis, University of Wisconsin-Madison (2015).

[18] T. Graham, B. Grinkemeyer, and et al., manuscript in preparation (2019).

[19] S. Zhang, F. Robicheaux, and M. Saffman, "Magic-wavelength optical traps for Rydberg atoms," Phys. Rev. A **84**, 043408 (2011).

[20] S. Zhang, "Trapping and Rydberg excitation of a single atom qubit in a blue detuned bottle beam," PhD thesis, University of Wisconsin-Madison (2012).

[21] S. de Leséléuc, D. Barredo, V. Lienhard, A. Browaeys, and T. Lahaye, "Analysis of imperfections in the coherent optical excitation of single atoms to Rydberg states," Phys. Rev. A **97**, 053803 (2018).

[22] Our expression for $T_{2,\mathrm{D}}$ is $\sqrt{2}$ larger than that in [27] where this dephasing mechanism was first pointed out.

[23] X. L. Zhang, A. T. Gill, L. Isenhower, T. G. Walker, and M. Saffman, "Fidelity of a Rydberg blockade quantum gate from simulated quantum process tomography," Phys. Rev. A **85**, 042310 (2012).

[24] M. Saffman, "Quantum computing with atomic qubits and Rydberg interactions: Progress and challenges," J. Phys. B **49**, 202001 (2016).

[25] L. S. Theis, F. Motzoi, F. K. Wilhelm, and M. Saffman, "A high fidelity Rydberg blockade entangling gate using shaped, analytic pulses," Phys. Rev. A **94**, 032306 (2016).

[26] X. L. Zhang, L. Isenhower, A. T. Gill, T. G. Walker, and M. Saffman, "Deterministic entanglement of two neutral atoms via Rydberg blockade," Phys. Rev. A **82**,

030306(R) (2010).

[27] T. Wilk, A. Gaëtan, C. Evellin, J. Wolters, Y. Miroshny-chenko, P. Grangier, and A. Browaeys, "Entanglement of two individual neutral atoms using Rydberg blockade," Phys. Rev. Lett. **104**, 010502 (2010).

[28] Supplementary material at ... which includes references [30–35].

[29] H. Levine, A. Keesling, G. Semeghini, A. Omran, T. T. Wang, S. Ebadi, H. Bernien, M. Greiner, V. Vuletić, H. Pichler, and M. D. Lukin, "Parallel implementation of high-fidelity multi-qubit gates with neutral atoms," arXiv: ??? (2019).

[30] M. Saffman and T. G. Walker, "Analysis of a quantum logic device based on dipole-dipole interactions of optically trapped Rydberg atoms," Phys. Rev. A **72**, 022347 (2005).

[31] M. Saffman, X. L. Zhang, A. T. Gill, L. Isenhower, and T. G. Walker, "Rydberg state mediated quantum gates and entanglement of pairs of neutral atoms," J. Phys.: Conf. Ser. **264**, 012023 (2011).

[32] K. Gillen-Christandl, G. Gillen, M. J. Piotrowicz, and M. Saffman, "Comparison of Gaussian and super Gaussian laser beams for addressing atomic qubits," Appl. Phys. B **122**, 131 (2016).

[33] I. I. Beterov, I. I. Ryabtsev, D. B. Tretyakov, and V. M. Entin, "Quasiclassical calculations of blackbody-radiation-induced depopulation rates and effective life-times of Rydberg nS, nP, and nD alkali-metal atoms with $n <= 80$," Phys. Rev. A **79**, 052504 (2009); "Erratum: Quasiclassical calculations of blackbody-radiation-induced depopulation rates and effective lifetimes of Rydberg nS, nP, and nD alkali-metal atoms with $n <= 80$," **80**, 059902 (2009).

[34] I. I. Beterov, M. Saffman, E. A. Yakshina, V. P. Zhukov, D. B. Tretyakov, V. M. Entin, I. I. Ryabtsev, C. W. Mansell, C. MacCormick, S. Bergamini, and M. P. Fedoruk, "Quantum gates in mesoscopic atomic ensembles based on adiabatic passage and Rydberg blockade," Phys. Rev. A **88**, 010303(R) (2013).

[35] M. Kwon, M. F. Ebert, T. G. Walker, and M. Saffman, "Parallel low-loss measurement of multiple atomic qubits," Phys. Rev. Lett. **119**, 180504 (2017).

SUPPLEMENTARY MATERIAL FOR RYDBERG MEDIATED ENTANGLEMENT IN A TWO-DIMENSIONAL NEUTRAL ATOM QUBIT ARRAY

In this supplementary material we reproduce Table I from the main text and provide explanations, additional measurements, and underlying calculations that support the error model. The error modeling largely follows earlier analyses[5, 23, 26, 30–32] supplemented by new material concerning atom position variations with respect to the Rydberg beam envelopes and the influence of laser phase noise on gate fidelity.

SM-I. ATOMIC PARAMETERS AND FINITE TEMPERATURE EFFECTS

Before proceeding with the individual errors we note that error averaging over the computational basis states, which is appropriate for characterizing the Rydberg C_Z fidelity, is the same as the error for the specific input state that is used to prepare a Bell state. Therefore we do not need to distinguish between error estimates for the C_Z gate and error estimates for preparing a Bell state.

To clarify this statement suppose the four computational basis states $|ij\rangle$ have associated C_Z gate errors ϵ_{ij}. The gate error averaged over the computational basis states is then $\epsilon_{C_Z} = (\epsilon_{00} + \epsilon_{01} + \epsilon_{10} + \epsilon_{11})/4$. When preparing the Bell state the two-qubit state that is input to the C_Z operation is $(|00\rangle + |01\rangle + |10\rangle + |11\rangle)/2$. The Bell state error probability due to the C_Z errors is therefore $\epsilon_{\text{Bell}} = \epsilon_{00}/4 + \epsilon_{01}/4 + \epsilon_{10}/4 + \epsilon_{11}/4 = \epsilon_{C_Z}$. An implicit assumption that justifies equivalence of errors is that there are no correlations between different error channels.

a.1 Ground-Rydberg Doppler dephasing

Rydberg excitation is performed with counterpropagating beams of different wavelengths so there is a wavenumber mismatch $k_{2\nu} = 2\pi/\lambda_1 - 2\pi/\lambda_2$. This leads to a stochastic phase for atoms that are Rydberg excited, spend a time t_{gR} in the Rydberg state, and then de-excited. This was originally pointed out in [27], although our analysis[22, 31] gives a smaller prediction for the magnitude of the phase error.

The average stochastic phase term can be expressed as $\langle e^{\imath\phi} \rangle = e^{-t_{\text{gR}}^2/T_{2,\text{D}}^2}$ with $T_{2,\text{D}} = \sqrt{2M_{\text{Cs}}/k_B T_a}/k_{2\nu}$. At the measured atomic temperature of $T_a = 15$ μK we find $T_{2,\text{D}} = 6$ μs. This effect limits the Bell fidelity to $F_{\text{Bell}}^{\max} = (1 + \langle e^{\imath\phi}\rangle)/2 = 0.987$ using $t_{\text{gR}} = 0.98$ μs. Our measurement of the ground-Rydberg coherence decay using a Ramsey experiment reveals a shorter coherence time of $T_{2,\text{gR}} = 4$ μs which would imply $F_{\text{Bell}}^{\max} = 0.971$. We do not use this value in the error table because the difference between $T_{2,\text{D}}$ and $T_{2,\text{gR}}$ is assumed due to other error mechanisms, including Rydberg radiative lifetime, atom position variations, and laser noise, that are separately included in the table.

a.2 Rydberg radiative lifetime

The lifetime of the Cs $66s$ state in a room temperature bath is calculated to be [33] $\tau = 130$ μs giving a spontaneous emission error for the gate of $\epsilon = e^{-t/\tau}/4$. The relevant time is that of the gate integrated Rydberg population which is 0 for state $|00\rangle$, t_π for state $|01\rangle$, t_{gR} for state $|10\rangle$, and t_{gR} for state $|11\rangle$ giving a total of $t = 2t_{\text{gR}} + t_\pi = 2.11$ μs. The error is then $\epsilon = 0.004$ which is small even for the relatively low excitation $n = 66$ state used here.

a.3 Rydberg motional dwell time

During the Rydberg excitation pulses the trap light is turned off. If the atom moves outside of the trapping region before the trap light is turned on again it will be lost, leading to an error. We estimate this error in terms of an effective motional lifetime which is the minimum distance the atom has to move to be lost $(d/2)$ divided by the average thermal velocity $v = \sqrt{k_B T_a/M}$. The atom motion is three dimensional, but the distance for trap loss is much longer in the axial direction, so we approximate this effect by setting the loss time to $\tau_{\text{motion}} = (d/2)/(\sqrt{2}v)$. With $d = 3.1$ μm and $T_a = 15$ μK we find $\tau_{\text{motion}} = 36$ μs. The error is the same as for a.2 with τ replaced by τ_{motion} giving $\epsilon = 0.014$.

a.4 Scattering from $7p_{1/2}$

Two-photon excitation is via the $7p_{1/2}$ state which has a radiative lifetime of $\tau_{7p} = 155$ ns. The one-photon detuning is $\Delta/2\pi = 680$ MHz. The probability of spontaneous emission in a π pulse when the one-photon Rabi frequencies are equal is $P_{\text{se}} = \frac{\pi}{2}\frac{1}{\tau_{7p}\Delta}$. Here we are neglecting corrections due to the hyperfine structure of the $7p_{1/2}$ state. The full expressions, including those corrections, can be found in [10].

Averaging over the input states we find the error

$$\epsilon = \frac{1}{4}\Big[0. \qquad\qquad (|00\rangle)$$

$$+ 2\frac{\pi}{2}\frac{1}{\tau_{7p}\Delta} \qquad\qquad (|01\rangle)$$

$$+ 2\frac{\pi}{2}\frac{1}{\tau_{7p}\Delta} \qquad\qquad (|10\rangle)$$

$$+ 2\frac{\pi}{2}\frac{1}{\tau_{7p}\Delta} + \frac{\pi}{2}\frac{1}{\tau_{7p}\Delta}\Big] \qquad (|11\rangle)$$

$$= \frac{7\pi}{8}\frac{1}{\tau_{7p}\Delta} = 0.004.$$

TABLE SM-I. Error budget for Rydberg C_Z gate and Bell state preparation using parameters from the Bell state experiment. The listed error values are for two atoms averaged over the four computational basis states. This is the same as Table I in the main text.

quantity	error	fidelity estimate
a) atomic parameters & finite temperature effects		
a.1) ground-Rydberg Doppler dephasing (calculated)	0.013	
a.2) Rydberg radiative lifetime (calculated)	0.004	
a.3) Rydberg motional dwell time (calculated)	0.014	
a.4) scattering $7p_{1/2}$ (calculated)	0.004	
a.5) blockade leakage (calculated)	0.001	
a.6) atom position in Rydberg beams (calculated)	0.035	
a.7) laser noise (estimated)	0.02	
	total 0.092	$F_{C_Z}^{-\text{SPAM}} = 0.908$
b) single qubit errors		
b.1) initial and parity global μwave pulses (measured)	0.008	
b.2) Stark μwave pulse (measured)	0.012	
	total 0.020	$F_{\text{Bell}}^{-\text{SPAM}} = 0.888$
c) SPAM errors		
c.1) atom preparation (measured)	0.01	
c.2) optical pumping (estimated)	0.01	
c.3) state measurement (measured)	3.0×10^{-4}	
	total 0.020	$F_{\text{Bell}} = 0.868$

In the contribution from the $|11\rangle$ state we include half of the blockaded excitation of the target atom since excitation by the first 459 nm photon is not blockaded.

a.5 Blockade leakage

Due to less than infinite blockade strength there is finite rotation of the blockaded state. The average error is [5] $\epsilon = \Omega_R^2/8\mathsf{B}^2$. The calculated blockade strength for Cs $66s$ at a distance of $R = \sqrt{2}d$ is $\mathsf{B}/2\pi = 45$ MHz which gives $\epsilon = 0.001$. Measurements of the blockade showed less than 0.02 leakage which is consistent with SPAM estiamtes given below.

a.6 Atom position in Rydberg beams

All the reported measurement results are averaged over multiple realizations and for each realization the atomic position is slightly different. Averaging over atomic positions leads to decay of coherent oscillations, an effect that was studied numerically in [32]. Here we calculate the expected errors and their uncertainties for π and 2π pulses. This contribution to the error budget, as well as the contribution from laser noise in the following section, has larger uncertainty then the other errors due to lack of precise knowledge of the optical parameters of the array. In particular the width and shape of the lines defining the trapping sites affect the atomic localization but are only known approximately.

The position distribution of a trapped atom at finite temperature can be modeled as a Gaussian with radial and axial localization parameters σ, σ_z and normalized distribution

$$\rho(\mathbf{r}) = \frac{1}{(2\pi)^{3/2}\sigma^2\sigma_z}e^{-(x^2+y^2)/(2\sigma^2)}e^{-z^2/(2\sigma_z^2)}.$$

The Rydberg beam field amplitudes relative to their values at the center of the beam are

$$f_j(\mathbf{r}) = \frac{e^{-(x^2+y^2)/w_j^2(z)}}{\sqrt{1 + z^2/L_{R_j}^2}}.$$

Here $w_j^2(z) = w_j^2(1 + z^2/L_{R_j}^2)$ are the z dependent beam waists, $L_{R_j} = \pi w_j^2/\lambda_j$ are the Rayleigh lengths, and $j = 1, 2$. We assume that the Rydberg beams are aligned with the origin of the atom distribution. If Ω_R is the two-photon Rabi frequency at the center of the beams then the position dependent Rabi frequency is $\Omega_R(\mathbf{r}) = \Omega_R f_1(\mathbf{r}) f_2(\mathbf{r})$.

Consider a 2π pulse of length t with the initial state $|i\rangle$. The average observed probability for the atom to be in $|1\rangle$ after the pulse is

$$\langle P_{|i\rangle}(t)\rangle = \int d\mathbf{r}\,\rho(\mathbf{r})\left\{\cos^2\left[\frac{\Omega_R t}{2}f(\mathbf{r})\right] + \frac{\Delta^2(\mathbf{r})}{\Omega_R^2(\mathbf{r}) + \Delta^2(\mathbf{r})}\sin^2\left[\frac{\Omega_R t}{2}f(\mathbf{r})\right]\right\}. \tag{1}$$

This expression includes the position dependent two-photon detuning $\Delta(\mathbf{r}) = \Delta_0 + \Delta_1 f_1^2(\mathbf{r}) + \Delta_2 f_2^2(\mathbf{r})$. Here

Δ_0 is a constant detuning and Δ_1, Δ_2 are Stark shift coefficients that depend on the beam intensities and detunings relative to the intermediate $7p_{1/2}$ state. Choosing $\Delta_0 = -(\Delta_1 + \Delta_2)$ ensures that an atom at trap center is resonantly excited.

The variance of the population error is

$$(\delta P)^2 = \left\langle \left[P_{|i\rangle}(t) - P_{\text{tar}} \right]^2 \right\rangle$$
$$= P_{\text{tar}}^2 + \left\langle \left[P_{|i\rangle}(t) \right]^2 \right\rangle - 2P_{\text{tar}}\langle P_{|i\rangle}(t)\rangle. \quad (2)$$

The pulse time t can be adjusted to minimize the difference between the observed average $\langle P_{|i\rangle}(t)\rangle$ and the target population P_{tar}. For a 2π pulse $P_{\text{tar}} = 1$ but, at finite temperature, there is no pulse time for which $\langle P_{|i\rangle}(t)\rangle = P_{\text{tar}}$. Nevertheless the time can be adjusted to minimize the difference between the target population and the observed average. For a 2π pulse $P_{\text{tar}} = 1$ and

$$(\delta P)^2 = 1 + \left\langle \left[P_{|i\rangle}(t) \right]^2 \right\rangle - 2\langle P_{|i\rangle}(t)\rangle. \quad (3)$$

Similar expressions govern the phase response. The amplitude of the initial state after a pulse of length t is

$$c(\mathbf{r}, t) = \cos\left[\sqrt{\Omega_R^2(\mathbf{r}) + \Delta^2(\mathbf{r})}\, t/2 \right]$$
$$- i \frac{\Delta(\mathbf{r})}{\sqrt{\Omega_R^2(\mathbf{r}) + \Delta^2(\mathbf{r})}} \sin\left[\sqrt{\Omega_R^2(\mathbf{r}) + \Delta^2(\mathbf{r})}\, t/2 \right] \quad (4)$$

The phase of the wavefunction is

$$\phi = -\tan^{-1}\left[\frac{\Delta(\mathbf{r})}{\sqrt{\Omega_R^2(\mathbf{r}) + \Delta_R^2(\mathbf{r})}} \tan\left[\frac{\sqrt{\Omega_R^2(\mathbf{r}) + \Delta^2(\mathbf{r})}}{2} t \right] \right]. \quad (5)$$

Expressing $\Omega_R(\mathbf{r})$ and $\Delta(\mathbf{r})$ in terms of f_1, f_2 and integrating over $\rho(\mathbf{r})$ as for the population distribution we calculate the phase error and uncertainty.

Perturbative analysis of the population variance in 2D for $\sigma \ll w$ shows that $(\delta P)^2 \sim (\sigma/w)^8$ so the standard deviation or uncertainty in the population scales as $(\sigma/w)^4$. This scaling highlights the sensitivity to finite beam size and the importance of low temperatures and tight localization of the atom. Sensitivity to variations in the local Rabi frequency and detunings can be minimized using adiabatic gate protocols (see, for example, [34]), but we have not done so here.

To determine the errors from atom position variations in 3D we have relied on numerical solutions of Eqs. (1-5). The atom localization parameters σ, σ_z were determined[18] using $T_a = 15$ μK, trap depth 285 μK, $d = 3.1$ μm, and line width $w_{\text{line}} = d/3.08 = 1.0$ μm to be $\sigma = 0.27$ μm, $\sigma_z = 1.47$ μm. The value of the line width that was used was increased by 7% from the value in the optical train to account for aperturing of the array light pattern on the objective lens aperture which caused broadening of the line.

With these parameters we find the results shown in Fig. SM-1. We see that the phase error as quantified
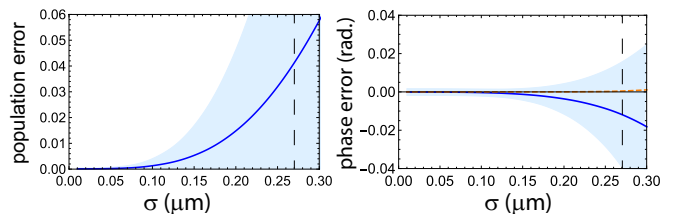

FIG. SM-1. Numerical solutions for the population and phase errors due to atom position variations after a 2π ground-Rydberg pulse. a) Population error with $\pm$ one standard deviation shown by the light blue shading. b) Phase error with $\langle \phi \rangle$ shown by the solid blue line, $\langle 1 - \cos(\phi) \rangle$ shown by the dashed orange line, and the standard deviation shown by the light blue shading. The vertical dashed lines show the expected value of σ for our trap parameters. Parameters: $w_1 = 2.25$ μm, $w_2 = 2.5$ μm, $\Omega_R/2\pi = 4.5$ MHz, $\Delta_1/2\pi = -2.7$ MHz, $\Delta_2/2\pi = 6.4$ MHz, $\Delta_0 = -(\Delta_1 + \Delta_2)$.

by $\langle 1 - \cos(\phi) \rangle$ is negligible. The expected population error is 0.04 but with a large uncertainty. Averaging over the input states we have a contribution to the gate error budget of $\epsilon = 3 \times 0.042/4 = 0.032$. The factor of 3 comes from the 2π pulse of state $|01\rangle$ and $\pi-$ gap $-\pi$ pulses for states $|10\rangle$ and $|11\rangle$ which we count as 2π pulses, neglecting any additional contribution from atom motion in the gap time.

The π rydberg pulse on the control atom also contributes an additional error since less than 100% population transfer from ground to Rydberg state implies a corresponding failure probability for blockade of the target qubit in the $|11\rangle$ state. The probability of populating the Rydberg state after a π pulse is

$$\langle P_{|R\rangle}(t) \rangle = \int d\mathbf{r}\, \rho(\mathbf{r}) \frac{\Omega_R^2(\mathbf{r})}{\Omega_R^2(\mathbf{r}) + \Delta^2(\mathbf{r})} \sin^2\left[\frac{\Omega_R t}{2} f(\mathbf{r}) \right] \quad (6)$$

The calculated population error for a π pulse using Eq. (6) is shown in Fig. SM-2. The error contribution is $\epsilon = 0.014/4 = 0.0034$ which we have combined with the 2π error of 0.032 to give a total of 0.035 due to atom position variations.

We emphasize that our confidence in this error estimate is lower than for other entries in the error model, due to lack of precise knowledge of trap parameters and atom localization. Furthermore these errors will be larger if the Rydberg beams are misaligned relative to the trap centers. There is also a correlation with the Rydberg atom motion (a.3) whereby a Rydberg excited atom will move and see a different beam amplitude under deexcitation. We have not included such effects in the analysis.

a.7 Laser noise

Laser noise due to intensity and phase fluctuations degrades the fidelity of coherent pulses. In addition to intensity noise that causes undesired Stark shifts, analogous to the effects of atom motion, phase noise arising
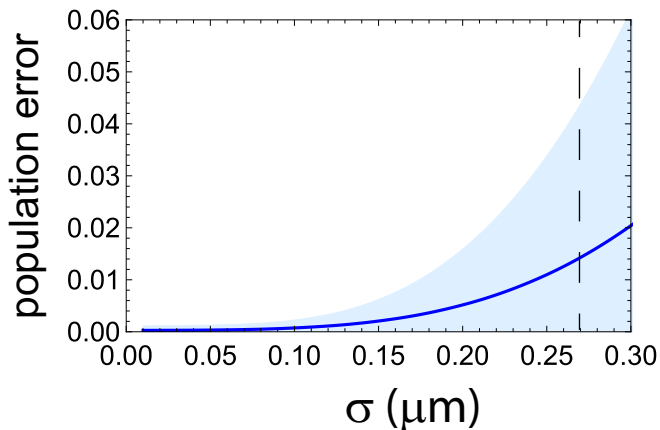
FIG. SM-2. Numerical solutions for the population error due to atom position variations after a π ground-Rydberg pulse with $\pm$ one standard deviation shown by the light blue shading. The vertical dashed lines show the expected value of σ. All other parameters the same as in Fig. SM-1.

from servo bumps has been shown to noticeably degrade Rabi oscillations[21]. The pulse errors can be significantly reduced by resonator filtering[14]. While we have demonstrated persistent coherence of ground-Rydberg oscillations in Fig. 2 without resonator filtering, it is also the case that significant day to day variations in Rabi oscillation amplitude were observed that could not always be directly correlated with the observable amplitude of servo bumps on the lasers.

Simulations we have performed by modeling servo bump noise as a superposition of frequency components with random phases confirm that the pulse errors are largest when the servo bump offset frequency is comparable to Ω_R. For integrated servo bump power of -20 dBr relative to the carrier we find population errors up to 0.04, and for -30 dBr errors up to 0.002. Temperature and current drifts in laser diodes result in changes in the laser mode structure and noise levels that also affect the experimental results, even without changes to lock parameters. This error is therefore difficult to quantify, but is certainly present since we have observed large changes in pulse errors with minor changes to the locking electronics parameters. A reasonable estiamte for this error is in between the -20 dBr and -30 dBr values given above. We have placed this error at 0.02 in the error model, but there are relatively large uncertainties.

a.8 Additional errors

There are two additional sources of error that are not included in the Table but will be relevant for future, higher fidelity gate demonstrations.

The first is the magnetic sensitivity of Rydberg states. Rydberg excitation is performed at a bias field of 0.6 mT which is well in the Paschen-Back limit for the Cs $66s_{1/2}$ state. Therefore the $m_j = -1/2$ state has a magnetic

sensitivity of approximately 14. GHz/T. The experiment is operated with synchronization to the 60 Hz AC power line to minimize magnetic noise. Although we have not carefully characterized magnetic noise at the location of the atoms, on the basis of measured atomic temperature and coherence times we estimate that the characteristic magnetic noise amplitude is not larger than 10^{-6} T. This implies a stochastic phase accumulation over the effective Rydberg excitation duration of a C_Z gate, which is $t_{\mathrm{gR}} = 0.98$ μs, of

$$\begin{aligned}\delta\phi &= 0.98 \ (\mu\mathrm{s}) \times 14. \ (\mathrm{GHz/T}) \times 10^{-6} \ (\mathrm{T}) \\ &= 0.014 \ (\mathrm{rad}).\end{aligned} \tag{7}$$

Averaging over input states this contribution should be multiplied by $1/2$ giving $\epsilon = 0.007$ which is negligible compared to other errors.

An additional potential source of error is the high sensitivity of Rydberg atoms to dc and ac electric fields. We have previously observed strong sensitivity of specific Rydberg states to background microwave fields when there are resonant transitions driven by cell phones or wi-fi networks. For the $66s_{1/2}$ state the lowest frequency transition to a $n'p$ state is at 12.5 GHz and the lowest frequency two-photon transition is 27. GHz for coupling to a $n's$ state and 11.7 GHz for coupling to a $n'd$ state. These frequencies are far from any wireless network bands and not expected to cause significant perturbations.

There is also sensitivity to time varying dc fields that are of concern up to a few MHz in frequency, corresponding to the bandwidth of the Rydberg pulses. The experiments are performed in glass cells with eight internal electrodes for field cancellation. The cells are manufactured by ColdQuanta, Inc. . The atomic array is 1 cm from the inside of the cell windows. Voltages generated by a low noise dc supply are used to cancel the background dc field as measured by Rydberg spectroscopy. When the field is minimized there is a quadratic maximum of the Rydberg energy and a zero derivative with respect to field strength which minimizes the Rydberg state sensitivity to fluctuations. The fields are checked every few months and significant changes relevant to the zero field condition have not been observed. We cannot presently exclude fluctuating fields that may cause Rydberg dephasing, but since we are unable to make a reliable estimate of the magnitude of this effect we have left it out of the error table.

SM-II. SINGLE QUBIT ERRORS

Single qubit rotations are performed with microwaves and focused Stark shifting lasers. These operations give additional errors that contribute to the infidelity of the Bell state and a CNOT gate but are separate from the fidelity of the Rydberg C_Z gate.

b.1 Global microwave pulses

The observed amplitude of microwave π pulses connecting the clock states is 0.988(4) for the control site and 0.985(4) for the target site is dependent on microwave power stability, frequency stability, phase noise, qubit coherence and SPAM errors. Subtracting the SPAM errors described below from the observed amplitudes we assign an error of 0.002 to a microwave π pulse. Since there are four such pulses in the Bell state protocol the total error is 0.008.

b.2 Local Stark shifted microwave pulses

To perform a local x-axis rotation gate with microwaves we use the decomposition

$$R_x(\theta) = R_y(\pi/2)R_z(\theta)R_y(-\pi/2).$$

The R_y operations are global microwave pulses and the R_z is a local Stark shifting pulse which we apply with the 459 nm Rydberg beam. A site which receives no Stark pulse only experiences two microwave rotations that cancel. The local gate in the Bell state preparation sequence is $R_\theta(\pi/2)$ about an angle θ in the azimuthal plane. This requires phase shifting the R_y pulses which was accomplished with a computer controlled signal generator.

The error for this operation is larger than for the global gates due to noise of the focused laser beam. We estimate this error to be 0.01 based on measured pulse amplitudes. Adding a 0.002 error for the non-addressed site gives an error for the Bell state protocol of 0.012.

SM-III. SPAM ERRORS

c.1 Atom preparation in traps

Atom preparation errors are due to retention loss during measurement to verify an atom is present. Mean and median values across the array are given in Fig. 1 in the main text. The measured loss for control and target sites was 0.005 for each site giving a 0.01 error.

This loss is partly due to measurement induced loss and partly due to background collisions at finite vacuum pressure. Our measured vacuum limited trap lifetime is about 30 s which implies a loss of 0.003 for a 100 ms duration double measurement. This loss contribution can be made negligible with faster measurements and improved vacuum conditions.

c.2 Optical pumping

The optical pumping error is difficult to disentangle from the atom preparation error since both contribute to a finite amplitude of microwave pulses. One measure of the pumping infidelity is the ratio of pumping to depumping times for preparation of $m_f = 0$ clock states. We have observed this ratio as low as 1/200 corresponding to an error of 0.005 per atom.

c.3 State measurement

State measurement errors were estimated by making Gaussian fits to the observed count distributions for atoms present and not present after pushing out atoms in $f = 4$ and defining the measurement error as the overlap of the distributions. The mean and median errors across the array are given in Fig. 1 in the main text. For the specific sites and measurement times used for the Bell state experiments we obtained lower measurement errors of 5×10^{-5} for the control site and 1×10^{-4} for the target site. We have used the average value of these errors in the table.

There is an additional error from blowing away atoms in $f = 4$, which may be less than 100% successful, may depump atoms to $f = 3$ instead of removing them from the trap, and may also cause loss of atoms in $f = 3$ with very low probability. On the basis of related studies with non-destructive state measurements[35] we estimate the errors from blow away are not larger than the overlap error derived from fitting the count disrtibutions. We have accordingly doubled the error estimate in the table to 3.0×10^{-4}.